Ferroelectric relaxor $Ba(Ti,Ce)O_3$

2002 J. Phys.: Condens. Matter 14 8901

(http://iopscience.iop.org/0953-8984/14/38/313)

INSTITUTE OF PHYSICS PUBLISHING JOURNAL OF PHYSICS: CONDENSED MATTER

J. Phys.: Condens. Matter **14** (2002) 8901–8912 PII: S0953-8984(02)31410-3

Ferroelectric relaxor Ba(Ti,Ce)O_3

Chen Ang[1,2], **Zhi Jing**[3] **and Zhi Yu**[2]

[1] Department of Physics, The University of Akron, Akron, OH 44325, USA
[2] Materials Research Laboratory, The Pennsylvania State University, University Park, PA16802, USA
[3] Department of Ceramics and Glass Engineering, University of Aveiro, 3810 Aveiro, Portugal

Received 30 November 2001
Published 12 September 2002
Online at stacks.iop.org/JPhysCM/14/8901

Abstract

The dielectric behaviour of $Ba(Ti_{1-y}Ce_y)O_3$ solid solutions ($y = 0$–0.3) has been studied. A small amount of Ce doping ($y = 0.02$) has weak influence on the dielectric behaviour of $Ba(Ti_{1-y}Ce_y)O_3$. With increasing Ce concentration, three phase transitions of pure $BaTiO_3$ are pinched into one rounded dielectric peak with frequency dispersion, and the relaxation time follows the Vogel–Fulcher relation. The evolution from a normal ferroelectric to a ferroelectric relaxor is emphasized. High strains ($S =\sim 0.1$–0.19%) with a small hysteresis under ac fields are obtained in ferroelectric relaxors $Ba(Ti_{1-y}Ce_y)O_3$. The physical mechanism of the relaxation process, the pinching effect of the phase transitions and their influence on the ferroelectric and electrostrictive behaviour are discussed.

1. Introduction

The 'ferroelectric relaxor' behaviour was first observed by Smolenskii *et al* [1] in Sn-doped $BaTiO_3$ (BTO). Later, the same phenomenon was found in $Pb(Mg_{1/3}Nb_{2/3})O_3$ (PMN) and $Pb(Sc_{1/2}Ta_{1/2})O_3$ (PST) compounds by the same group [2]. As concerns the mechanism of the ferroelectric relaxor behaviour, the main effort has been focused on lead-based complex-perovskite ABO_3 compounds, such as PMN, PST and (Pb, La)(Zr, Ti)O_3, since the 1980s [3–6]. To date, several models have been proposed to explain the physical nature of the ferroelectric relaxor behaviour [4–9]; however, the understanding of the physical picture of ferroelectrics relaxor is still a challenging subject. One of the barriers for this is probably the complicated crystalline structure and the occupancy of the hetrovalent ions at B-sites in these compounds [10]. Hence, some authors suggested that systems with simple crystalline structure, Li-doped $KTaO_3$ [10] and Bi-doped $SrTiO_3$ [11], which also display typical ferroelectric relaxor behaviour, might be good model systems for exploring the physical mechanism of ferroelectrics relaxor.

In fact, BTO doped with impurities, such as Sn [1], Hf [12], Ce [13], Y [14] and Zr [15, 16], possesses simple crystalline structure and shows ferroelectric relaxor behaviour. Obviously, detailed studies on BTO-based ferroelectrics relaxor can provide more experimental data in

addition to those from the lead-containing systems, and hence are helpful to understand the physical nature of the ferroelectric relaxor.

In addition, high piezoelectric and electrostrictive properties have recently been achieved in a series of Pb-containing ferroelectrics relaxor near the 'morphotropic phase boundary' (MPB) in the form of single crystals [17–19]. This could find wide applications in actuators, sensors etc. Due to the toxicity of lead, lead-free materials are desirable. Among several groups of lead-free candidate materials for high strain actuation applications, BTO is one of the most promising materials [20]. The high strain ($\sim$1%) was observed in tetragonal BTO along the [001] direction. However the strain versus electric field shows a large hysteresis, which blocks practical applications [20]. This means further modifications on pure BTO are needed. It is well known that the impurity doping is an effective way to improve the performance of electronic ceramics. In fact, it is reported that high strain with almost hysteresis-free behaviour can be obtained in Zr-doped BTO [21, 22].

Among BTO-based ferroelectrics relaxor, the ferroelectric/dielectric behaviour of Ce-doped BTO has recently received much attention due to both fundamental and application interests [23–26]. In a previous study of Ce-doped BTO [13, 26], the synthesis and the ferroelectric relaxor behaviour of some compositions of $Ba(Ti_{1-y}Ce_y)O_3$ ceramics were briefly reported. In this paper, we report the evolution from a normal ferroelectric to a ferroelectric relaxor in detail by extending the compositions to lower Ce concentrations. The physical mechanism of the relaxation process is briefly discussed. High strain ($S =\sim$ 0.16–0.19%) with small hysteresis under ac fields is observed. The physical mechanism of the relaxation process, the pinching effect of the phase transitions and their effect on the ferroelectric and electrostrictive behaviour are discussed.

2. Experimental procedure

Ceramics with the nominal compositions $Ba(Ti_{1-y}Ce_y)O_3$ with $y = 0$, 0.02, 0.06, 0.1, 0.2, 0.3, 0.33, 0.4 and 0.5 were synthesized by the mixed oxide method. The raw materials $BaCO_3$ (>99.5%, May & Baker Ltd), CeO_2 (>99.99%, Johnson Matthey GmbH) and TiO_2 (>99.8%, Johnson Matthey GmbH) were weighed according to the nominal compositions. The mixtures were wet mixed in alcohol on a planetary mill with agate balls for 6 h and calcined at 1200 °C for 4 h. The calcined powders were milled again for 6 h. After drying, the powders were isostatically pressed into discs under 300 MPa. Finally, the discs were sintered in air at 1530–1550 °C for 6 h, and furnace cooled.

The x-ray diffraction (XRD) analysis was carried out to determine the phase assemblage and lattice parameters of the samples by using Cu Kα radiation (Rigaku) at room temperature, with 2θ angles between 20° and 125° and the scanning speed of 1° min^{-1}.

The silver electrodes were pasted and then fired at 650 °C. The dielectric properties were measured with an HP4284A LCR meter and a Solartron 1260 impedance analyser in the temperature range 12–700 K, under an ac electric field of 1 V mm^{-1}. The strain as a function of electric field was measured at room temperature by a modified Sawyer–Tower circuit and linear variable differential transducer (LVDT) driven by a lock-in amplifier.

3. Results

3.1. Phase assemblage and crystalline structure

$Ba(Ti_{1-y}Ce_y)O_3$ ($0 \leqslant y \leqslant 0.5$) samples were examined by XRD. The results indicate that single-phase $Ba(Ti_{1-y}Ce_y)O_3$ solid solutions with a solubility limit $y = 0.3$ were

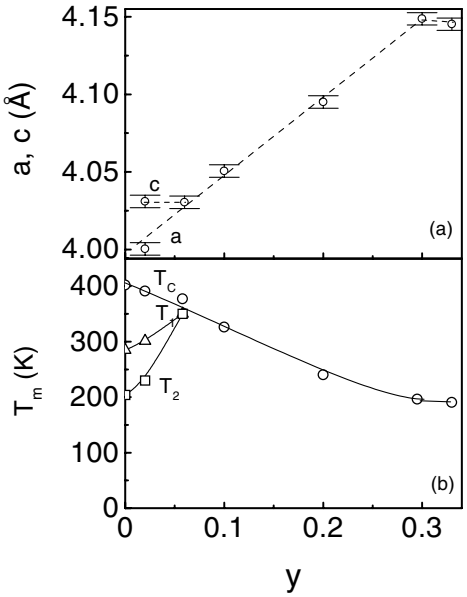

Figure 1. (a) The variation of the lattice parameters of the $Ba(Ti_{1-y}Ce_y)O_3$ ceramics as a function of Ce content y. (b) The variation of T_c ($T_{\varepsilon m}$), T_1 and T_2 at 10 kHz as a function of Ce content y.

identified [26]. The lattice parameters were calculated by the least squares method for the samples within the solid solution limit and a diphasic sample with $y = 0.33$. The variation of the lattice parameters as a function of Ce content is shown in figure 1(a). In the present work, the sample with $y = 0.02$ can be well indexed with the tetragonal symmetry. However, the samples with $y \geqslant 0.06$ are better indexed by the cubic symmetry. The lattice parameter of the samples with $y \geqslant 0.06$ is increased monotonically with increasing Ce content in the range $0.06 \leqslant y \leqslant 0.3$, but remains almost constant for $y \geqslant 0.3$, which confirms that the limit of the solid solubility of Ce^{4+} in BTO is $y = 0.3$. In the following, we focus on the dielectric behaviour of $Ba(Ti_{1-y}Ce_y)O_3$ within the limit of solid solubility ($y \leqslant 0.3$).

3.2. Temperature dependence of the dielectric behaviour

The temperature dependence of the real (ε') and imaginary parts (ε'') of the dielectric permittivity of $Ba(Ti_{1-y}Ce_y)O_3$($0 \leqslant y \leqslant 0.3$) at 1, 10 and 100 kHz is shown in figure 2. For $y = 0.02$, three dielectric peaks were observed at 391, 301 and 230 K, which are originated from phase transitions from a cubic paraelectric to a tetragonal ferroelectric (at T_c), and then to an orthorhombic ferroelectric (at T_1), and finally to a rhombohedral ferroelectric (at T_2), similar to those of pure BTO. However, T_c of pure BTO is shifted to a lower temperature and T_1 and T_2 to higher temperatures by the substitution of Ce ions for Ti ions. This is the so-called pinched phase transition as in Zr-, Sn-and Hf-doped BTO [27]. For $y = 0.02$, the dielectric peak at T_c appears relatively sharp and the peak temperature is independent of the measuring frequencies, similar to those observed in pure BTO. With increasing Ce substitution level, the three phase transitions are continuously pinched. Up to $y = 0.1$, the three phase transitions corresponding to pure BTO merge into one round ε peak, and the temperature ($T_{\varepsilon m}$) where the maximum of dielectric constant (ε_m) occurs is dependent on the measuring frequencies.

Upon further increasing Ce content, two common features can be observed in the dielectric response of $Ba(Ti_{1-y}Ce_y)O_3$ ($y \geqslant 0.2$).

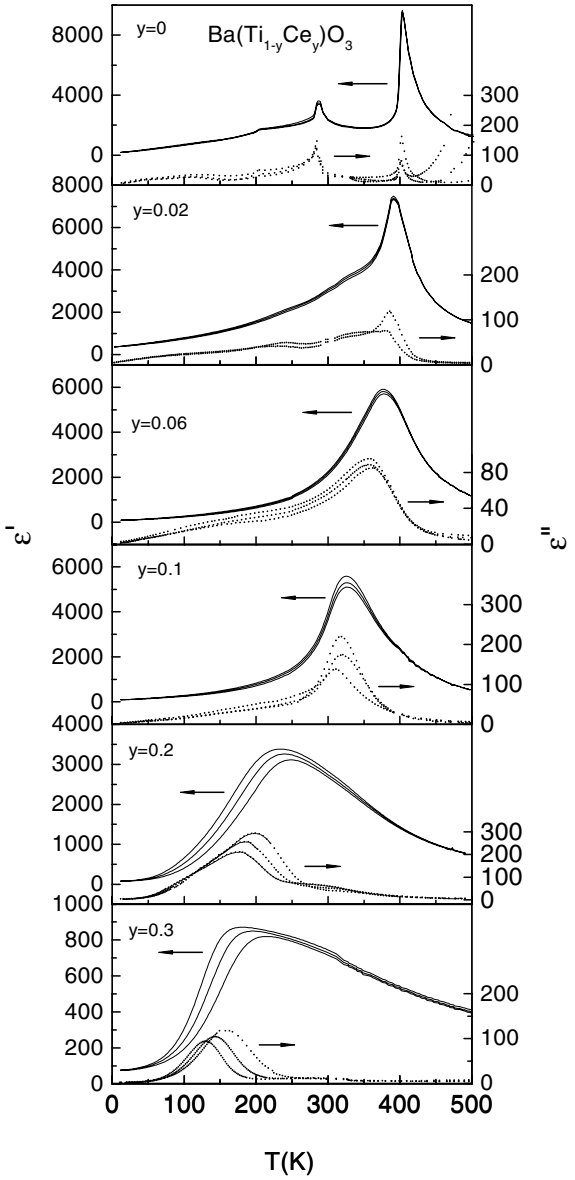

Figure 2. Temperature dependence of ε' and ε'' of the $Ba(Ti_{1-y}Ce_y)O_3$ ceramics with $y = 0$, $y = 0.02$, $y = 0.06$, $y = 0.1$, $y = 0.2$ and $y = 0.3$ at 1, 10, and 100 kHz. (ε': from top to bottom; ε'': from top to bottom for $y \leqslant 0.06$, from left to right for $y \geqslant 0.1$).

(1) The ε peak becomes more and more rounded, and ε_m decreases with increasing Ce content.
(2) Strong frequency dispersion was observed around the rounded ε peak, with $T_{\varepsilon m}$ being shifted to higher temperatures with increasing frequency.

Based on the dielectric response mentioned above, $Ba(Ti_{1-y}Ce_y)O_3$ ($0 \leqslant y \leqslant 0.3$) solid solutions can be accordingly classified into three groups: region I, $y \leqslant 0.02$; region II, $0.06 \leqslant y \leqslant 0.1$; region III, $0.2 \leqslant y \leqslant 0.3$. A normal ferroelectric behaviour is observed in region I, similar to that of pure BTO [27]. In region II, only one rounded dielectric peak

with very small frequency dispersion is found in $\varepsilon\prime$.Inregion III, the diffuse phase transition with obvious frequency dispersion is observed with further increasing Ce content, displaying a typical ferroelectric relaxor behaviour. The results of the three regions show the evolution from a normal ferroelectric to a ferroelectric relaxor with increasing Ce concentration.

The variation of the phase transition temperatures ($T_c/T_{\varepsilon m}$, T_1 and T_2) as a function of Ce content at 10 kHz is shown in figure 1(b). T_c (or $T_{\varepsilon m}$) decreases almost linearly for $y \leqslant 0.3$. However, T_1 and T_2 increase with Ce content below $y = 0.06$. The shifting rates of Ce doping at Ti sites are ~ -7, $\sim +11$ and $\sim +24$ K mol% $^{-1}$, for T_c (T_m), T_1 and T_2, respectively. This phase diagram also shows that the pinched phase transitions occur at $y = 0.06$.

Comparing figure 1(b) with figure 1(a) and figure 2, it can be seen that the crystalline symmetry is tetragonal for $y = 0.02$ and cubic for $y \geqslant 0.06$ at room temperature, and the unit cell increases with increasing Ce concentration in the solid solution range. Correspondingly, the dielectric response in figure 2 exhibits three dielectric peaks for $y = 0.02$, and one pinched dielectric peak for $y \geqslant 0.06$, and the ferroelectric relaxor behaviour becomes more pronounced with increasing Ce concentration. The correlation between the crystalline structure and the dielectric behaviour is presented.

3.3. Characterization of the ε peaks on the high temperature side

For a normal ferroelectric, the Curie–Weiss law

$$1/\varepsilon = (T - T_0)/C \qquad (T > T_c) \tag{1}$$

is followed, where T_0 is the Curie temperature and C is the Curie–Weiss constant. Figure 3 shows the inverse ε as a function of temperature at 10 kHz and the fits to the experimental data by equation (1). It was found that for the samples with low Ce concentration, e.g. $y = 0.02$, the dielectric constant follows the Curie–Weiss law. However, a deviation from the Curie–Weiss law is found with increasing Ce concentration. A parameter, ΔT_m, is defined to describe the deviation degree of ε from the Curie–Weiss law as the following:

$$\Delta T_m = T_{dev} - T_c \tag{2}$$

where T_{dev} is a temperature at which ε starts to deviate from the Curie–Weiss law.

In the literature [28], a modified Curie–Weiss law was proposed to describe the diffuseness of the phase transition as

$$1/\varepsilon - 1/\varepsilon_m = (T - T_{\varepsilon m})^{\gamma}/C_1 \tag{3}$$

where γ and C_1 are assumed to be constant, and $1 < \gamma < 2$. The limiting values $\gamma = 1$ and 2 reduce the expression to the Curie–Weiss law valid for the case of a normal ferroelectric and to the quadratic dependence valid for an ideal ferroelectric relaxor, respectively [2]. The fitting curves are shown in figure 4, and the parameters are listed in table 1.

The diffuseness of the phase transition can be described by an empirical parameter ΔT_{dif}, defined as

$$\Delta T_{dif} = T_{0.9\varepsilon_m(100\ \mathrm{Hz})} - T_{\varepsilon_m(100\ \mathrm{Hz})} \tag{4}$$

i.e., the difference between $T_{0.9\varepsilon_m(100\mathrm{Hz})}$ (the temperature corresponding to 90% of the maximum of dielectric constant (ε_m) in the high temperature side) and $T_{\varepsilon_m(100\ \mathrm{Hz})}$ (T_{ε_m} at 100 Hz).

On the other hand, the degree of relaxation behaviour can be described by a parameter ΔT_{relax}, which is defined as

$$\Delta T_{relax} = T_{\varepsilon_m(100\ \mathrm{kHz})} - T_{\varepsilon_m(100\ \mathrm{Hz})}. \tag{5}$$

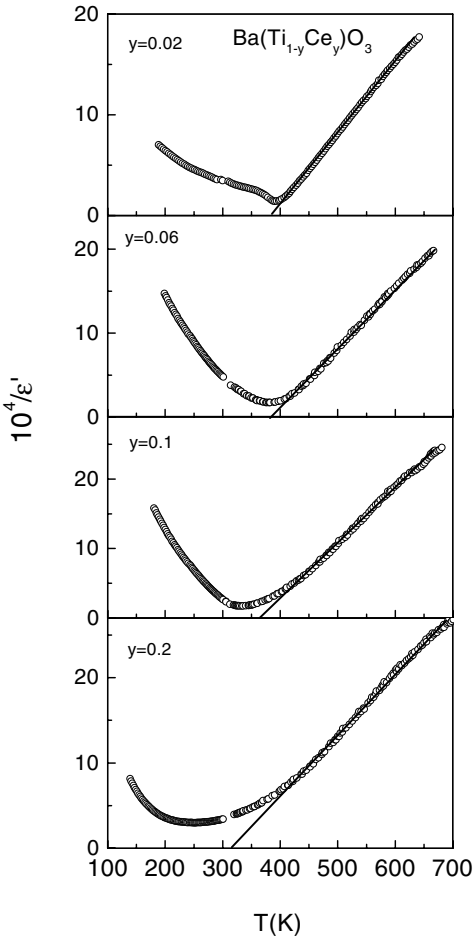

Figure 3. The inverse dielectric constant $(1/\varepsilon)$ as a function of temperature at 10 kHz for the $Ba(Ti_{1-y}Ce_y)O_3$ ($y = 0$, 0.06, 0.1 and 0.2) ceramics and the fit to the Curie–Weiss law (O, experimental data; solid lines, fitting curves).

Table 1. The Curie temperature (T_0), Curie constant (C) and the parameters C, T_0, $T_{\varepsilon m}$, ΔT_m, γ, ΔT_{dif} and ΔT_{relax} for $Ba(Ti_{1-y}Ce_y)O_3$ ($y = 0$–0.2).

		$y = 0$	$y = 0.02$	$y = 0.06$	$y = 0.1$	$y = 0.2$
T_c (or T_m) (K)		404	391	381	334	250
Curie–Weiss law	T_0 (K)	394	387	388	364	311
	C (10^5 K)	1.36	1.40	1.38	1.27	1.42
	ΔT_m (K)	∼2	30	40	84	145
γ		∼1.19	∼1.43	∼2	∼1.82	∼2
ΔT_{dif} (K)		3	11	20	20	44
ΔT_{relax} (K)		∼0	∼1.4	∼1.4	∼1.6	∼10

The experimental data were characterized by using equations (1)–(5) and all the parameters (C, T_0, ΔT_m, $T_{\varepsilon m}$, γ, ΔT_{dif} and ΔT_{relax}) were obtained for $Ba(Ti_{1-y}Ce_y)O_3$ ($y = 0$–0.2) and are listed in table 1.

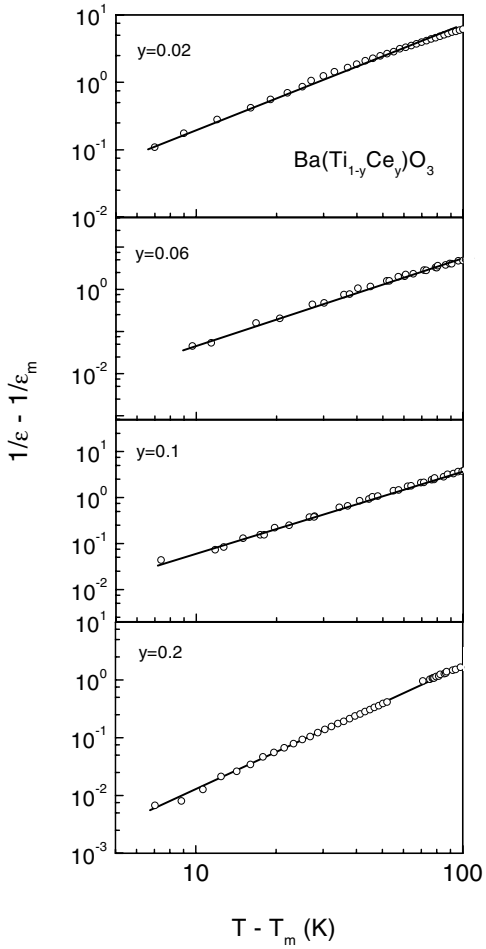

Figure 4. The curves of $(1/\varepsilon - 1/\varepsilon_m)$ versus $(T - T_m)$ for the Ba $(Ti_{1-y}Ce_y)O_3$ ceramics with $y = 0$, 0.06, 0.1 and 0.2 (○, experimental data; solid lines, fitting to equation (3). $T_{\varepsilon m}$ is the temperature corresponding to the dielectric constant maximum, ε_m).

The above empirical characterizations with the Curie–Weiss law (ΔT_m) and the parameters ΔT_{relax}, ΔT_{dif} and γ show that ε of the compositions with $y \leqslant 0.02$ follows the Curie–Weiss law, and the deviation from a normal ferroelectric is very small. This indicates that the compositions with $y \leqslant 0.02$ exhibit the normal ferroelectric behaviour. The Curie–Weiss temperature T_0 is 4 K lower than T_c for $y = 0.02$, showing a first-order ferroelectric-like phase transition. For $y = 0.06$ and 0.1, obvious deviations from the Curie–Weiss law, and large diffuseness of the phase transition, are observed; however, the frequency dispersion (ΔT_{relax}) is small. Furthermore, ε follows the Curie–Weiss law only at temperatures much higher than T_m for $y = 0.2$ and 0.3, and the parameters ΔT_{relax} and γ become significantly larger than that of $y = 0.1$. The diffuseness of the dielectric peak becomes more and more pronounced with increasing Ce content. The strong frequency dispersion observed in samples with $y = 0.2$ and 0.3 is characterized by an increase in ΔT_{relax} values.

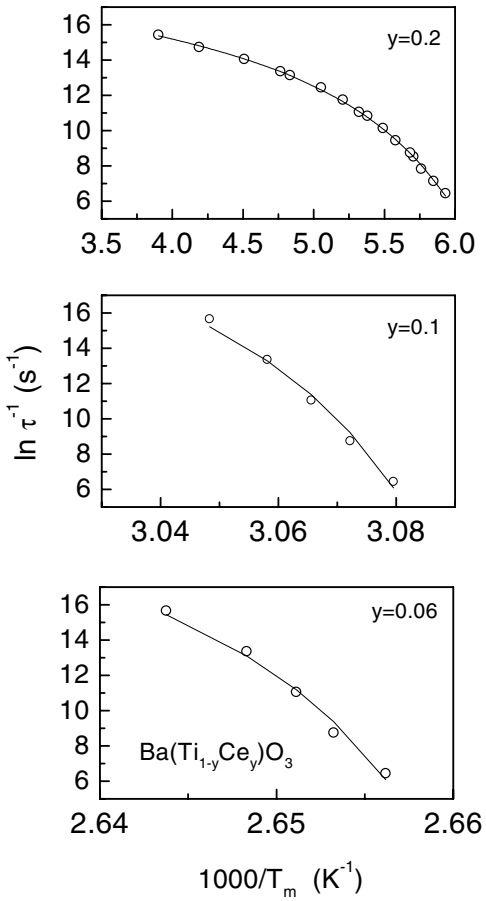

Figure 5. Relaxation time τ versus $1/T$ curve for $Ba(Ti_{1-y}Ce_y)\ TiO_3$ ($y = 0.06$, 0.1 and 0.2) (O, the experimental data; solid curves, fitting to the Vogel–Fulcher relation).

3.4. Temperature dependence of the relaxation time

The relaxation time (τ) obtained from the imaginary part of the complex permittivity for the samples with $y = 0.06$, 0.1 and 0.2 as a function of inverse temperature is shown in figure 5. It should be pointed out that, although the frequency dispersion is very small for $y = 0.06$ and 0.1, for example, the ΔT_{relax} value as defined by equation (4) is ∼1.4 K for $y = 0.06$ as the frequency increases from 100 Hz to 100 kHz, the relaxation time τ does not follow the Arrhenius law, but it follows well the empirical Vogel–Fulcher relation [29],

$$\tau = \tau_0 \exp\{E/[k_B(T - T_{VF})]\} \tag{6}$$

where τ_0 is the pre-exponential term, E is the hindering barrier, T_{VF} is the Vogel–Fulcher temperature and k_B is the Boltzmann constant. The fitting parameters are listed in table 2.

3.5. Strains

The field dependence of the bipolar and unipolar strains of Ce-doped BTO is shown in figure 6. For the samples with low Ce doping level ($y \leqslant 0.16$), the unipolar strain levels are in the range of 0.10–0.19% at 60 kV cm^{-1}, and the strain hysteresis is small. The strain levels are

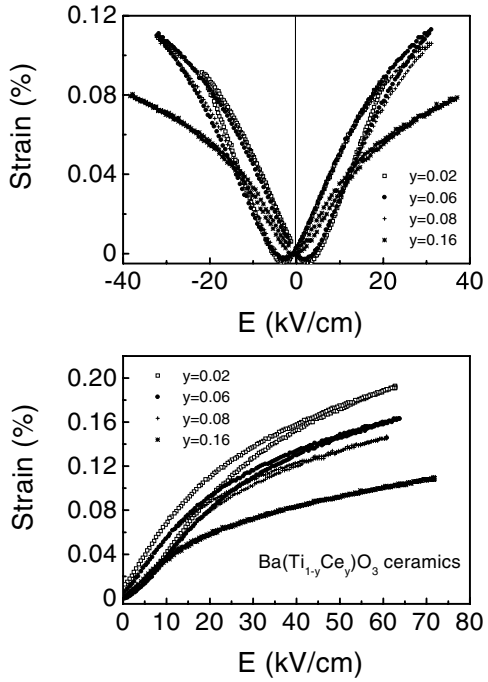

Figure 6. Bipolar and unipolar strains of $Ba(Ti_{1-y}Ce_y)O_3$ ($y = 0.02$, 0.06, 0.08 and 0.16) samples measured at room temperature (∼295 K) and 0.2 Hz.

Table 2. The activation energy (E), pre-exponential factor (τ_0) and characteristic temperature (T_{VF}) obtained by fitting to the Vogel–Fulcher relation for the $Ba(Ti_{1-y}Ce_y)O_3$ solid solutions.

	$y = 0.06$	$y = 0.1$	$y = 0.2$
τ_0 (s)	6.91×10^{-12}	6.91×10^{-12}	9.24×10^{-9}
E (meV)	3.9	7.6	27
T_{VF} (K)	374.1	320.1	138.7

reasonably high for ceramics as compared with lead-containing materials, such as Pb(Zr, Ti)O_3 (PZT), and Pb(Mg, Nb)O_3–$PbTiO_3$ (PMN-PT) ceramics [18]. The highest strain is 0.19% at ∼60 kV cm^{-1} for the $y = 0.02$ sample in Ce-doped BTO. At the pinched point $y = 0.06$, similar strain behaviour is observed, but the strain level slightly decreases, and a value of 0.16% was obtained. With increasing Ce doping concentration, the strain level gradually decreases, and simultaneously the hysteresis decreases. These results indicate that this system is a promising candidate for actuator applications, and it would be interesting to grow single crystals of Ce-doped BTO, in which much higher electrostrictive effect is expected.

4. Discussion

4.1. Pinching effect of the phase transitions and strains

From figure 2, it can be seen that the paraelectric to ferroelectric phase transition temperature T_c of pure BTO is decreased and the two lower phase-transition temperatures (tetragonal to orthorhombic T_1 and orthorhombic to rhombohedral T_2) increase with increasing Ce content.

The average shifting or pinching rates of the Ce doping at Ti sites are large, ~ -7, $\sim +11$ and $\sim +24$ K mol% $^{-1}$, for T_c, T_1 and T_2, respectively. At $y = 0.06$, three phase transitions merge into one round peak, i.e., the three phase transitions of BTO were pinched by Ce doping. With further increasing Ce concentration, more rounded and diffuse dielectric peaks are observed. The crossover from a normal ferroelectric to a ferroelectric relaxor occurs. At the pinched point, different phase transitions join together, implying that several phases with small difference in the free energy could coexist in the same composition. From this point of view, the pinching region is similar to the so-called MPB region in PZT and related solid solutions [27].

As mentioned above, the high piezoelectric and electrostrictive properties in the Pb-based ferroelectric relaxors are obtained near the MPB and it is generally recognized that near the MPB, the coexistence of several phases with small difference in the free energy is helpful to enhance the piezoelectric performance.

If this can be applied to other systems, for example, Ce-doped BTO solid solutions, the high piezoelectric and electric-field-induced strain effect could be expected around the pinching point, i.e., at $y = 0.06$. However, in the present work, a reasonably high strain level with small hysteresis is obtained at $y = 0.02$ and the strain level decreases monotonically with increasing Ce concentration. This indicates that in BTO solid solutions around the pinched point of the three phase transitions no obvious enhancement in the piezoelectric performance is observed.

It is reported that pure BTO single crystals possess a strain level as high as $\sim 1\%$ with obvious hysteresis. This is attributed to the tetragonality of BTO, $(c - a)/a \sim 1\%$, and the significant contribution from the domain reorientation. Based on this fact, it is not difficult to understand the strain behaviour of doped BTO, as well as its high strain level as compared with those PZT ceramics and electrostrictive ceramics PMN-PT [18].

With increasing Ce doping concentration, the $(c - a)/a$ ratio decreases to 0.77% at $x = 0.02$, to 0.04% at $x = 0.06$ [13]. As x exceeds 0.06, the system can be indexed to a cubic symmetry. In this way the tetragonality decreases, and thus leads to a lower piezoelectric strain. It will be interesting to study the relationship among the tetragonality, strain levels and hysteresis for other element substitutions at Ba sites or Ti sites in BTO.

In addition, it should be pointed out that by Ce doping, a crossover from a typical ferroelectric behaviour to 'ferroelectric relaxor' behaviour occurs; this indicates that the long range ferroelectric order (i.e., the macrodomain) is broken into microdomain states. The results above show that in a ferroelectric relaxor state, a smaller strain and less hysteresis are observed as compared with the ferroelectric BTO; this implies that the reorientation of the microdomain under a unipolar electric field in a ferroelectric relaxor contributes less to the field-induced strain. Further study is necessary in better understanding the strain mechanism of this system.

4.2. Evolution from a normal ferroelectric to a ferroelectric relaxor

The ferroelectric relaxor behaviour can be induced in doped BTO as mentioned in the introduction. Although the physical mechanism of the ferroelectric relaxor is not fully understood to date, the existence of the micropolar clusters in the material is recognized to play an important role in the occurrence of the ferroelectric relaxor behaviour [4, 5, 11].

When Ti ions are substituted by Ce ions, the structure and the ferroelectricity of BTO are modified. On the one hand, Ce-doped BTO can be taken as a solid solution of BTO and $BaCeO_3$ compounds. However, $BaCeO_3$ is a nonferroelectric. Because Ce ions possess a larger ionic radius (0.087 nm) than Ti ions (0.0605 nm) [32], the substitution of Ce ions tends to make the distance between off-centre Ti dipoles larger and thus weakens the correlation between these dipoles, which is supported by the experimental facts that the lattice parameter and volume of the cell increase with increasing Ce concentration. Ferroelectric domains are

destroyed and micropolar clusters are formed. In other words, the mismatch in size between Ti ions and Ce ions might cause substantial distortion of the oxygen octahedra, giving rise to the local electric and strain fields. These local electric and strain fields are usually random in nature and tend to break the macro ferroelectric domains into micropolar clusters.

Consequently, the ferroelectric/dielectric behaviour of $Ba(Ti_{1-y}Ce_y)O_3$ depends on the competition between the long range ferroelectric order owing to strong correlation of the off-centre Ti dipoles and the random fields induced by the Ce doping. When Ce concentration is small ($0 < y < 0.06$), the ferroelectricity is dominant. When the Ce concentration is high enough ($y \geqslant 0.2$), the existence of the static random fields leads to the destruction of the long-range ferroelectric order and the micropolar clusters form, hence, the relaxor behaviour occurs in the heavily Ce-doped BTO ceramics.

5. Conclusions

The dielectric behaviour of the $Ba(Ti_{1-y}Ce_y)O_3$ ceramics was studied in a wide composition range ($0 \leqslant y \leqslant 0.3$). The evolution from a normal ferroelectric to a ferroelectric relaxor was observed with increasing Ce concentration. The characterization of the dielectric behaviour with empirical parameters (ΔT_m, γ, ΔT_{dif} and ΔT_{relax}) indicates that the diffuseness and the relaxation degree increase with increase in Ce content, so does the deviation from the classical Curie–Weiss law. A high strain level (0.1–0.19% in the form of ceramics) with a small hysteresis is observed, indicating that the system is a promising lead-free electrostrictive material.

Acknowledgments

One of the authors (Zhi Jing) would like to thank the PRAXIS XXI, FCT (Portuguese Foundation for Science and Technology) for the financial support.

References

[1] Novosil'tsev N S and Khodakov A L 1956 *Zh. Tekhn. Fiz.* **26** 310 (Engl. transl. 1956 *Sov. Phys.–Tech. Phys.* **1** 306)
[2] Smolenskii G A and Agranovskaya A I 1958 *Sov. Phys.–Tech. Phys.* **3** 1380
Smolenski G A 1970 *J. Phys. Soc. Japan Suppl.* **28** 26
[3] Setter N and Cross L E 1980 *J. Appl. Phys.* **51** 4356
[4] Yao X, Chen Z L and Cross L E 1984 *J. Appl. Phys.* **54** 3399
[5] Cross L E 1987 *Ferroelectrics* **76** 241
[6] Viehland D, Jang S J, Cross L E and Wuttig M 1990 *J. Appl. Phys.* **68** 2916
[7] Westphal V, Kleemann W and Glinchuk M D 1992 *Phys. Rev. Lett.* **68** 847
[8] Vugmeister B E and Rabitz H 1998 *Phys. Rev.* **57** 7581
[9] Pirc R and Blinc R 1999 *Phys. Rev.* **60** 13 470
[10] Toulouse J, Vugmeister B E and Pattnaik R 1994 *Phys. Rev. Lett.* **73** 3467
[11] Chen A, Zhi Y and Zhi J 2000 *Phys. Rev.* B **61** 957
Chen A, Zhi Y, Vilarinho P M and Baptista J L 1998 *Phys. Rev.* B **57** 7403
Chen A, Zhi Y, Lunkenheimer P, Hemberger J and Loidl A 1999 *Phys. Rev.* B **59** 6670
[12] Payne W H and Tennery V J 1965 *J. Am. Ceram. Soc.* **48** 413
[13] Zhi Y, Chen A, Zhi J, Vilarinho P M and Baptista J L 1997 *J. Phys.: Condens. Matter* **9** 3081
[14] Zhi J, Chen A, Zhi Y, Vilarinho P M and Baptista J L 1998 *J. Appl. Phys.* **84** 983
[15] Hennings D and Schnell A 1997 *J. Am. Ceram. Soc.* **65** 1982
Ravez J and Simon A 1997 *Eur. J. Solid. State Inorg. Chem.* **34** 1199
[16] Zhi Y, Chen A, Guo R and Bhalla A S 2002 *J. Appl. Phys.* **92** 2655
[17] Park S E and Shrout T R 1997 *J. Appl. Phys.* **82** 1804

[18] Kuwata J, Uchino K and Nomura S 1982 *Japan. J. Appl. Phys.* **21** 1298
[19] Liu S F, Park S E, Shrout T R and Cross L E 1999 *J. Appl. Phys.* **85** 2810
[20] Wada S, Suzuki S, Noma T, Suzuki T, Osada M, Kakihana M, Park S E, Cross L E and Shrout T R 1999 *Japan. J. Appl. Phys.* **38** 5505
[21] Rherig P W, Park S E, McKinstry S T, Messing G L, Jones B and Shrout T M 1999 *J. Appl. Phys.* **86** 1657
[22] Zhi Y, Guo R and Bhalla A S 2000 *Appl. Phys. Lett.* **77** 1535
Schreinemacher B and Schreinemacher H 1994 *J. Eur. Ceram. Soc.* **13** 81
[23] Park Y and Kim Y 1995 *J. Mater. Res.* **10** 2770
[24] Makovec D, Samardaija Z and Kolar D 1996 *J. Solid State Chem.* **123** 30
[25] Makovec D, Samardaija Z and Kolar D 1997 *J. Am. Ceram. Soc.* **80** 45
[26] Chen A, Zhi Y, Zhi J, Vilarinho P M and Baptista J L 1997 *J. Eur. Ceram. Soc.* **17** 1217
[27] Jaffe B, Cook W and Jaffe H 1971 *Piezoelectric Ceramics* (London: Academic)
[28] Uchino K and Nomura S 1982 *Ferroelectr. Lett.* **44** 55
[29] Vogel H 1921 *Z. Phys.* **22** 645
Fulcher G 1925 *J. Am. Ceram. Soc.* **8** 339
[30] Gervais F 1984 *Ferroelectrics* **53** 91
[31] Müller K A and Berlinger W 1986 *Phys. Rev.* B **34** 6130
[32] Shannon R D 1976 *Acta Crystallogr.* A **32** 751